

Lightning over Three Large Tropical Lakes and the Strait of Malacca: Exploratory Analyses

RONALD L. HOLLE

Vaisala, Inc., Tucson, Arizona

MARTIN J. MURPHY

Vaisala, Inc., Louisville, Colorado

(Manuscript received 19 January 2017, in final form 30 August 2017)

ABSTRACT

Lightning stroke density measured by the Global Lightning Dataset (GLD360) has shown several strong maxima around the globe. Several of these extremes are located over large tropical water bodies surrounded by terrain features. Four prominent maxima are examined and compared in this study: Lake Maracaibo in South America, the Strait of Malacca in equatorial Asia, Lake Victoria in East Africa, and Lake Titicaca in South America. Specifically, the authors observe that all four water bodies exhibit sustained maxima in lightning occurrence all night, the peak lightning frequency occurs very late at night or the following morning at three of the four sites, and the nocturnal maxima are out of phase at the four locations even though the afternoon maxima over the surrounding terrain all occur between 1500 and 1700 local solar time. The meteorological factors affecting the diurnal cycle of lightning occurrence over these four water bodies, which are all adjacent to mountains, are explored in this study.

1. Introduction

In the tropics, the diurnal cycle is a very strong regulator of precipitation in general, and convective precipitation and lightning specifically. In fact, Venugopal et al. (2016) show that the diurnal frequency tops the power spectrum of tropical lightning occurrence, and in the power spectrum of rainfall, the diurnal cycle is second only to seasonal frequencies. The amplitude and phase of the diurnal cycle are affected at the broad, global scale by the land–ocean contrast. Kikuchi and Wang (2008), using precipitation data from the Tropical Rainfall Measuring Mission (TRMM), defined a coastal regime in which the diurnal cycle on the land side shows inland-directed propagation between 0900 and 2100 local solar time (LST), under the influence of sea breezes with the daytime heating of nearby higher terrain also possibly drawing the sea breeze deeper inland. On the sea side, propagation was found to be offshore, and maximum precipitation was overnight or in the morning hours. Land breezes have been found to be weaker than sea breezes (e.g., Mapes et al. 2003a). However, cooler

and therefore stronger outflows from land-based moist convection during the afternoon, and/or gravity waves generated by daytime convection along and over elevated terrain, are better associated with an organized seaward-propagating nocturnal maximum in convective precipitation.

At finer spatial scales, the amplitude and phase of the diurnal cycle are influenced by the local environment, particularly the contrast between water bodies large enough to be relevant at meso- α to meso- β scales and surrounding terrain features. Three such features have been the subject of recent studies where the diurnal cycle of lightning has been described at least in part: Lake Maracaibo in northwestern Venezuela (Albrecht et al. 2016; Muñoz et al. 2016; Virts et al. 2013a; Bürgesser et al. 2012), the Strait of Malacca in Southeast Asia (Venugopal et al. 2016; Virts et al. 2013a, b; Albrecht et al. 2016), and Lake Victoria in east-central Africa (Albrecht et al. 2016; Bürgesser et al. 2013). In general, these three locations all exhibit nocturnal maxima in lightning activity over the water bodies and mid- to late-afternoon maxima over the surrounding land areas.

In those cases where a mechanism of the diurnal cycle around these three water bodies has been discussed, the

Corresponding author: ron.holle@vaisala.com

DOI: 10.1175/MWR-D-17-0010.1

© 2017 American Meteorological Society. For information regarding reuse of this content and general copyright information, consult the [AMS Copyright Policy](http://www.ametsoc.org/PUBSReuseLicenses) (www.ametsoc.org/PUBSReuseLicenses).

low-altitude circulation tends to dominate the discussion. Around Lake Maracaibo, [Albrecht et al. \(2016\)](#) show daytime and nighttime wind roses from three sites: one at the north end of the lake, one on the east shore, and one near the southwest corner of the lake. From the nighttime wind roses, it appears that there is some case to be made for nocturnal low-level convergence. However, it should be noted that, *on average*, the nighttime winds at the southwest corner are roughly parallel to the lake shore, not truly offshore, while *on average*, the daytime winds at the north end of the lake are from the north and northeast (lake directed). With regard to the Strait of Malacca and Lake Victoria, [Albrecht et al. \(2016\)](#) cite generally convergent offshore breezes or land breezes. Similarly, [Virts et al. \(2013b\)](#) implicate the convergence of land breezes from both sides of the Strait of Malacca in the development of the nocturnal maximum in lightning activity there, although they also mention the gravity wave mechanism of [Mapes et al. \(2003a\)](#) at least with respect to the offshore propagation of thunderstorms from the Malaysian Peninsula and the island of Sumatra. [Bürgesser et al. \(2013\)](#), leaning on an earlier, regional climate modeling study by [Song et al. \(2004\)](#), also cite land breezes as the forcing mechanism behind the nocturnal lightning maximum over Lake Victoria.

The emphasis on low-level forcing, particularly land breezes, in the foregoing literature ignores a couple of key points. First, [Mapes et al. \(2003a\)](#) discussed an asymmetry between sea and land breezes in the tropics, with land breezes being typically much weaker. This is due to primarily the relatively weak nocturnal temperature contrast between land and water in the deep tropics. Second, as discussed in detail below, there is a rather significant phase delay between the decay of afternoon thunderstorms over the surrounding land and the nocturnal maxima in lightning density over the water bodies. It is postulated that, even if cool thunderstorm outflow, as opposed to land breeze, were the dominant means of forcing nocturnal thunderstorm development over the water bodies, then the water bodies might exhibit a single dominant pulse in thunderstorms, initiated near sunset and peaking shortly thereafter, rather than sustained all-night thunderstorm activity with maxima deep into the nighttime hours or even near sunrise the following morning.

The foregoing literature all relies on lightning information from one or both of two sources. The first is the Lightning Imaging Sensor (LIS) on the TRMM satellite and its predecessor, the Optical Transient Detector ([Boccippio et al. 2002](#); [Mach et al. 2007](#)). In either case, any given thunderstorm is only observed for about 90 s at most, and thus, long periods of observations must

be assembled into composites in order to obtain a reasonable representation of the diurnal cycle, but the advantage of the satellite data is the high total lightning detection efficiency (DE). The second source is the World Wide Lightning Location Network (WLLN). This is a continuously operating ground-based lightning locating system, such that the diurnal cycle is sampled continuously with no need to do the type of very long-term aggregation that is necessary with LIS. Continuous ground-based datasets therefore offer the possibility of doing detailed examinations of the diurnal cycle as well as intraseasonal and/or interannual time scales. WLLN, however, only detects about 10% of lightning and has a bias toward the detection of oceanic lightning over land-based lightning ([Abarca et al. 2010](#); [Rudlosky and Shea 2013](#)). In this study, the use of a different ground-based network is introduced, that of the Global Lightning Dataset (GLD360) ([Said et al. 2013](#)), which is both continuously observing and has a DE of around 80% in the areas of study ([Said and Murphy 2016](#)) and no known land–ocean detection bias ([Said et al. 2013](#)).

The primary objective of this paper is a more in-depth analysis of the diurnal cycle of lightning activity over and around four tropical water bodies. These include the three already mentioned: Lake Maracaibo, the Strait of Malacca, and Lake Victoria, but in addition, Lake Titicaca in the Andes is included, which, as will be demonstrated, also has a nocturnal lightning maximum despite its rather different situation from the other three locations. Three key observations that have not received specific attention in the prior literature are highlighted about the nocturnal lightning activity at all four of these locations: 1) the sustainment of lightning activity throughout the nighttime hours and, in fact, into the following morning; 2) the delayed peak of lightning activity until very late at night or sometimes after sunrise the following morning at all but Lake Titicaca; and 3) the wide variation in phasing of the nocturnal maxima over these four water bodies, even though the afternoon maxima over the surrounding terrain are very well phase matched at about 1500–1700 LST at all four locations. These key observations are then placed in the context of the mechanisms of diurnal variability described in the prior literature, particularly [Mapes et al. \(2003a\)](#).

2. GLD360 data

GLD360 is a ground-based lightning detection network providing worldwide coverage with the expectation of substantially uniform and high cloud-to-ground (CG) flash DE ([Mallick et al. 2014a](#); [Poelman et al. 2013](#); [Pohjola and Mäkelä 2013](#); [Said et al. 2013](#)). In this study, GLD360 data from the four calendar years of 2012–15

are utilized. On 18 August 2015, an updated location algorithm increased the NLDN-relative CG flash DE of GLD360 from 63% (Said et al. 2013) to 81%, and it was verified that the system has essentially no day–night variation in DE (Said and Murphy 2016). All of the data used in this study prior to 18 August 2015 were reprocessed using the updated algorithm. Ground truth validations prior to the algorithm upgrade by Mallick et al. (2014b) measured an absolute CG flash DE of 67% with a stroke DE of 37% in Florida, and by Poelman et al. (2013) measured a CG flash DE of 96% in Belgium. Based on a rudimentary argument using the preupgrade flash and stroke DE values, we can expect the postupgrade stroke DE to be roughly 56%.

In this study, stroke density is computed using a $5 \text{ km} \times 5 \text{ km}$ grid. Given that there are some differences in the validated DE of GLD360 in different parts of the world, and that the available literature to date does not yet include a global model showing the estimated performance of GLD360 in our areas of interest, no DE corrections are applied to the stroke counts or stroke densities. Additionally, although GLD360 does detect some cloud lightning (Said and Murphy 2016), there is, as yet, no way to identify the cloud lightning, so any cloud pulses that are detected are included in the stroke densities presented in this study. In addition to stroke density, the time of day when the maximum lightning density occurs is computed on a $20 \text{ km} \times 20 \text{ km}$ grid in order to minimize statistical noise and emphasize the important patterns of behavior. Hovmöller-like diagrams are also computed along cross sections through the four selected water bodies.

3. Characteristics of the four water bodies and their surroundings

The geographical situations surrounding the four water bodies are shown in Fig. 1. All but the Lake Victoria maps in Fig. 1 start at sea level, while the highest elevation varies in order to provide maximum resolution within each map. Each panel of Fig. 1 also shows two analysis areas: a polygon or rectangle containing the land areas that are considered to be relevant around each water body, and then each water body itself, outlined by its shoreline.

- (i) Lake Maracaibo has a maximum north–south extent of 200 km and east–west extent of 120 km. It is actually a bay that opens to the ocean on the north side, and its surface is at sea level. Its basin is surrounded by high mountains that begin to rise from a mostly flat plain 30–150 km away in all directions but north. The highest elevation within the

analysis area is 5007 m in the Merida Andes to the southeast. The lake has a maximum depth of only about 33 m (Table 1) in the east-central part (National Geospatial-Intelligence Agency 1988). The water temperature averages about 30°C with little seasonal variation (Berghuis 1995). Lake Maracaibo has a very large annual total average stroke density, identified as the world's largest by Albrecht et al. (2016).

- (ii) The Strait of Malacca is one of the busiest shipping lanes in the world and extends from Singapore on the southeast to the Indian Ocean to the northwest. The mountains of Sumatra on the west side reach a peak altitude of 3466 m, while those to the east only reach 1000 m or more in a small area of north-central Malaysia. The strait is only about 75 km across from Singapore to Kuala Lumpur but gradually opens to 300 km on the northwest end. It is shallow, like Lake Maracaibo, with depths of less than about 75 m (Table 1) until it opens to the Indian Ocean at the northwest end. The average sea surface temperature is about 30°C most of the year (NOAA/OAR/ESRL PSD 2017).
- (iii) Lake Victoria is the largest lake in Africa, largest tropical lake in the world, and second largest freshwater lake in the world by area. Unlike the previous two cases, Lake Victoria is in an elevated basin at about 1100 m above sea level. However, similar to both Lake Maracaibo and the Strait of Malacca, Lake Victoria has only a maximum depth of about 80 m (Anyah 2005). The surface water temperature ranges from 24° to 28°C on average (Anyah 2005 and references therein), with warmer water along the west side (Sun et al. 2015). The mountains of the Eastern Rift Valley on the Kenyan side of the lake reach an altitude of 5188 m, while the high terrain of the Western Rift Valley extends to more than 3000-m altitude and includes several other large north–south lakes.
- (iv) Lake Titicaca is at 15°S latitude, farther from the equator than Lake Maracaibo. The lake surface is at an altitude of 3812 m, considerably higher than the other three water bodies. However, it is surrounded by mountains well in excess of 6000-m altitude, and thus the altitude differential between the lake and the surrounding terrain is similar to that of both Lake Victoria and the Strait of Malacca. Lake Titicaca is deeper than the other three water bodies, with a maximum depth of 284 m, and it is also considerably colder due to its altitude, with water surface temperatures varying between 11° and 15°C during the course of the year, as measured from a station on the northwest

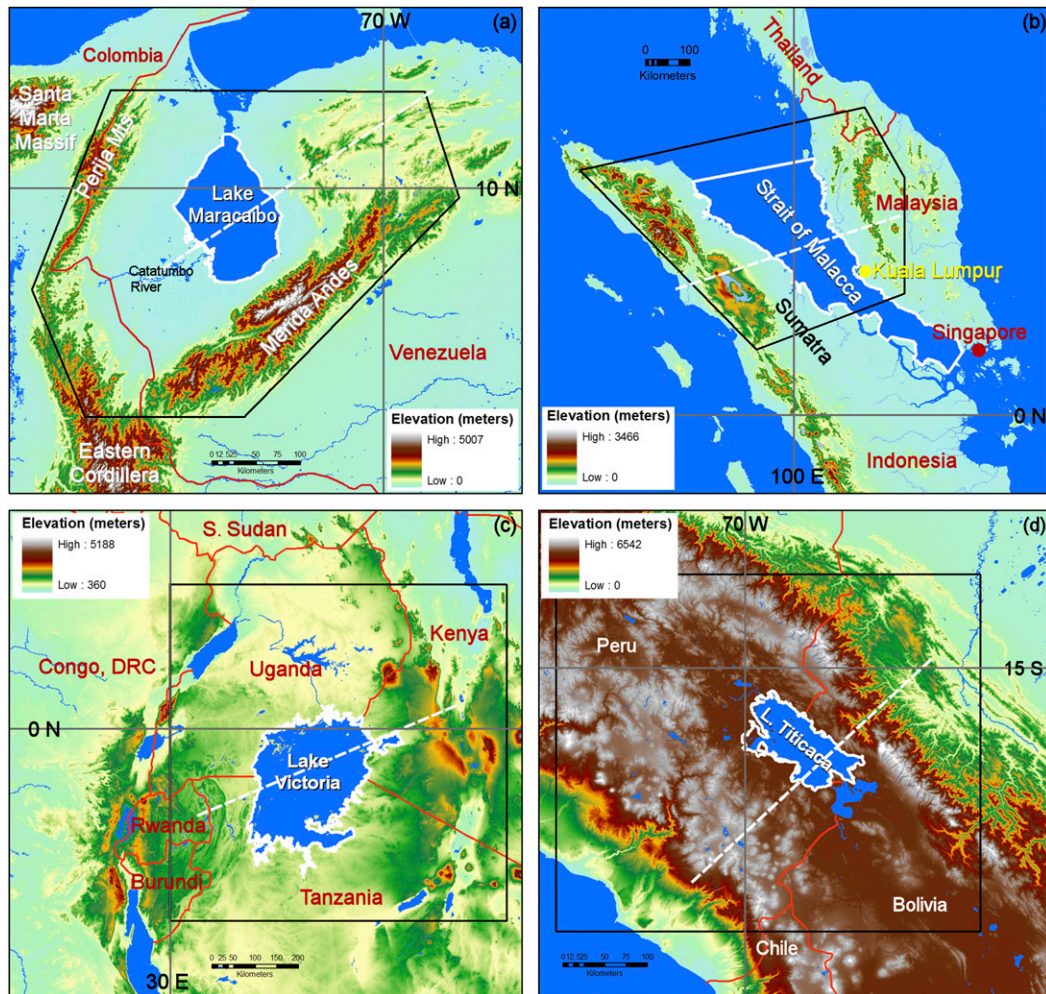


FIG. 1. Topography of the four study areas over and surrounding (a) Lake Maracaibo, (b) Strait of Malacca, (c) Lake Victoria, and (d) Lake Titicaca. Black polygons in (a) and (b), and black rectangles in (c) and (d) bound the exterior analysis areas. Water bodies are surrounded by white lines, country boundaries are in red, and dashed white lines are centers of cross sections shown in Fig. 7. Major mountain ranges and a river are identified in (a) and Kuala Lumpur is shown in (b).

side (Delclaux et al. 2007 and references therein). Lake Titicaca is the highest navigable lake in the world and the largest lake in South America by water volume. The highest mountain ridges are to

the northeast and southeast of the lake on a portion of the Andes whose northeastern flank drops within 200 km into the plains leading to the Amazon basin.

TABLE 1. Altitude, latitude, maximum depth, water temperature, number of strokes per year, area, and stroke density per year of the four water bodies outlined in white in Fig. 1.

| | Lake Maracaibo | Strait of Malacca | Lake Victoria | Lake Titicaca |
|---|-----------------|--------------------------|---------------|------------------------|
| Altitude | 0 m | 0 m | 1134 m | 3812 m |
| Latitude | 10°N | 4°N | 1°S | 16°S |
| Max depth | 33 m | 75 m | 80 m | 284 m |
| Water temperature | 30°C | 30°C | 24°–28°C | 11°–15°C |
| Temperature reference | Berghuis (1995) | NOAA/OAR/ESRL PSD (2017) | Anyah (2005) | Delclaux et al. (2007) |
| Strokes yr ⁻¹ | 1 954 779 | 6 015 216 | 703 263 | 83 188 |
| Area (km ²) | 12 110 | 83 810 | 68 220 | 6984 |
| Strokes km ⁻² yr ⁻¹ | 161 | 72 | 10 | 12 |

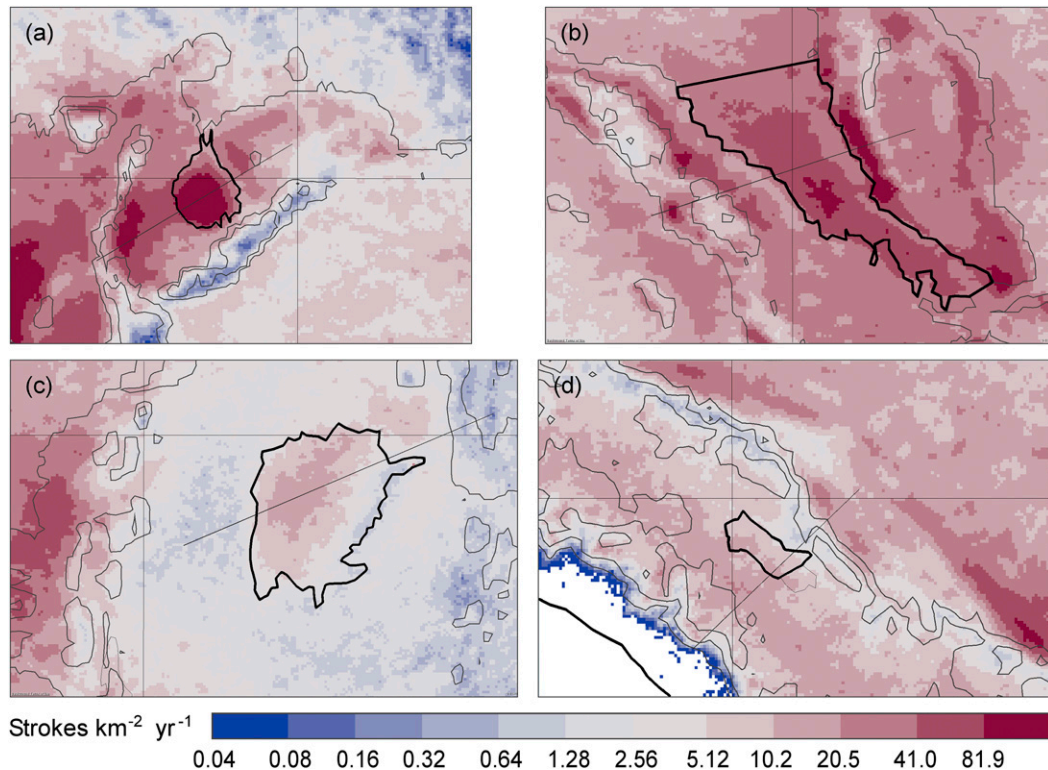


FIG. 2. Annual stroke density detected by the GLD360 over and surrounding (a) Lake Maracaibo, (b) Strait of Malacca, (c) Lake Victoria, and (d) Lake Titicaca in a $5 \text{ km} \times 5 \text{ km}$ grid from 2012 to 2015. Terrain altitude contours are shown in black at altitudes of 0, 1000, and 2000 m in (a),(b); 1000, 2000, and 3000 m in (c); and 2500, 3500, and 4500 m in (d); and the water bodies are outlined in black. The Pacific Ocean coastline is in black in (d). Black southwest–northeast lines indicate locations of the cross sections in Fig. 7.

4. Annual stroke densities

Table 1 summarizes the general characteristics of the four water bodies and their average annual lightning activity, in order of discussion in the following paragraphs and sections. The lightning stroke counts given in Table 1 are the per-year averages during 2012–15 as measured by GLD360, and the stroke densities are simply these stroke counts divided by the areas of the respective water bodies highlighted in Fig. 1.

Lake Maracaibo has an average stroke density of $161 \text{ strokes km}^{-2} \text{ yr}^{-1}$ (Table 1). While there are large lightning stroke densities over the slopes of several mountain ranges surrounding the lake, none are as large and strong as over the water surface. In contrast, the highest mountains have the lowest stroke densities (blue). In particular, there is a significant minimum in lightning density directly over the Merida Andes, which run from northeast to southwest close to the southeast side of the lake, and other density minima are located over the Eastern Cordillera, Perijá Mountains, and Santa Marta Massif. Outside the lake itself, stroke densities are largest on the slopes of the mountain

ranges rather than over them (López and Holle 1986; Holle 2014). We speculate that this could either be due to a lack of deep moisture in convective updrafts that start at the middle troposphere rather than near the surface, as noted by Houze (2012) based on Frei and Schär (1998), or it could be that the convection simply starts so early in the day over the highest terrain that the temperature differential, and thus the CAPE, has insufficient time to rise enough to yield strong convection. Some indication of this effect is included in MacGorman et al. (2007) where cloud-to-ground flash rates were found to increase with the thickness of the radar-observed 30-dBZ layer. Stolz et al. (2015) also found a relationship of lightning occurrence with the height of 30-dBZ echoes and warm cloud depth. However, neither of these studies specifically addressed the topic of reduced flash rates for storms that initiate at higher altitudes such as those located around the periphery of the four water bodies examined here. Such an analysis of the relevant dynamic and thermodynamic impacts is warranted in future studies.

The Strait of Malacca annual map in Fig. 2b indicates a lightning maximum over the strait and several stronger

maxima on the slopes of surrounding mountains. The average density (Table 1) is $72 \text{ strokes km}^{-2} \text{ yr}^{-1}$, less than half of the Lake Maracaibo mean, located over the slope of the topography near Kuala Lumpur, Malaysia, on the eastern shore of the Strait of Malacca. Additional stroke density maxima are located on the eastern shores of Sumatra and the Malaysian Peninsula, north of Singapore, and at several locations on the western shore of Sumatra. Minima are apparent over the highest elevations of Sumatra and Malaysia as indicated in Fig. 2b.

The broader region surrounding Lake Victoria in Fig. 2c includes one of the highest annual stroke densities in the world located several hundred kilometers to the west of the lake, west of the Mitumba Mountains in the Democratic Republic of the Congo (Albrecht et al. 2016), and a much less intense maximum over the lake. The massive region of high stroke density exceeding $10 \text{ strokes km}^{-2} \text{ yr}^{-1}$ to the west extending from the western slopes of the mountain ranges into the Congo basin is not over the mountains themselves. Note in Table 1 that the lake is large, resulting in the overall area-average stroke density over the lake of only $10 \text{ strokes km}^{-2} \text{ yr}^{-1}$, much smaller than Lake Maracaibo (161) and the Strait of Malacca (72). As noted around Lake Maracaibo, the highest peaks and ridges to the east of the lake, and of the Western Rift Valley, have lightning densities below $1 \text{ stroke km}^{-2} \text{ yr}^{-1}$ but larger densities exceeding $5 \text{ strokes km}^{-2} \text{ yr}^{-1}$ along their slopes.

The lightning density maxima near Lake Titicaca extend northwest–southeast on both the east and west sides of the lake (Fig. 2d). The largest stroke density on the west side is between the highest altitudes and the lake, as found for the other water bodies. However, the largest stroke density to the east of Lake Titicaca is east of the Andes over the foothills. GLD360 detects $83810 \text{ strokes yr}^{-1}$ over the lake, considerably fewer than over the lakes at lower altitudes. However, it is a much smaller lake by area than the other water bodies studied here, so the area-average stroke density of $12 \text{ km}^{-1} \text{ yr}^{-1}$ (Table 1) is actually higher than over Lake Victoria. Minima in stroke density are found over the Pacific Ocean and adjacent coastal plain where cold water offshore inhibits convection. The areas in Fig. 2d in white over the Pacific Ocean and the adjacent plains had no detected lightning at all during the 4-yr period. Another minimum is observed over the highest portions of the Andes, in an orientation from northwest to southeast.

5. Monthly variations

Over Lake Maracaibo, lightning frequency is not uniform through the year (Fig. 3a). Lightning is most frequent from August to October, and a secondary peak

occurs during April and May. The overlake maxima lag the exterior polygon by a month in both peaks. A distinct lightning minimum prevails from November to March. The Caribbean low-level jet is cited by Muñoz et al. (2016) as having the dominant seasonal-scale influence over thunderstorm activity in the region, with the annual migration of the ITCZ, in turn, modifying the Caribbean low-level jet. Land and water areas show proportionally the same trends. The number of hours and days with lightning over Lake Maracaibo is very large. GLD360 detects an average of 304 days yr^{-1} when there is at least 1 stroke over the lake (83% of possible days). This daily total agrees with the TRMM LIS climatology of Albrecht et al. (2016) who found an average of 297 days yr^{-1} with lightning. The range is $287\text{--}332 \text{ days yr}^{-1}$ during the 2012–15 GLD360 data period. At least 1 stroke is detected over the lake during 2658 hr^{-1} (30% of possible hours). From April to November, every month has at least 27 days with lightning over the lake. Even in the relatively weak lightning months of June and July, more than enough strokes occur such that there is at least 1 stroke day^{-1} .

Figure 3b shows monthly lightning counts over the Strait of Malacca to exhibit two maxima: one in March–May and the other in October and adjacent months. Land and water areas show the same trends. These periods are likely related to the passage of the equatorial trough across the region due to the migration of the summer and winter monsoon. This is consistent with the changes in mean wind direction from northeasterly to southwesterly in May and back to northeasterly in September (Fujita et al. 2010).

Lake Victoria has two seasonal maxima in lightning: one in October–December and the other in February–April (Fig. 3c). Both lake and adjacent land areas show the same trends. The two maxima are likely related to the passage of the equatorial trough across the region (Chamberlain et al. 2014 and references therein). A similar seasonal behavior is seen in the precipitation in this region (Chamberlain et al. 2014).

Lake Titicaca has a strong seasonal variation in its thunderstorm activity with a significant maximum between November and March and very little lightning from May to July (Fig. 3d). Both land and lake areas have the same trends. The strong annual cycle is associated with the transport of mid- to upper-level moisture from the east through the setup of the Bolivian high late in the Southern Hemisphere spring (Garreaud 1999; Jones and Carvalho 2002). The South American low-level jet is a significant source of moisture along the east slope of the Andes, but evidently only up to about 2500-m altitude. At higher altitudes, the exact position of the Bolivian high regulates the flow of moisture into

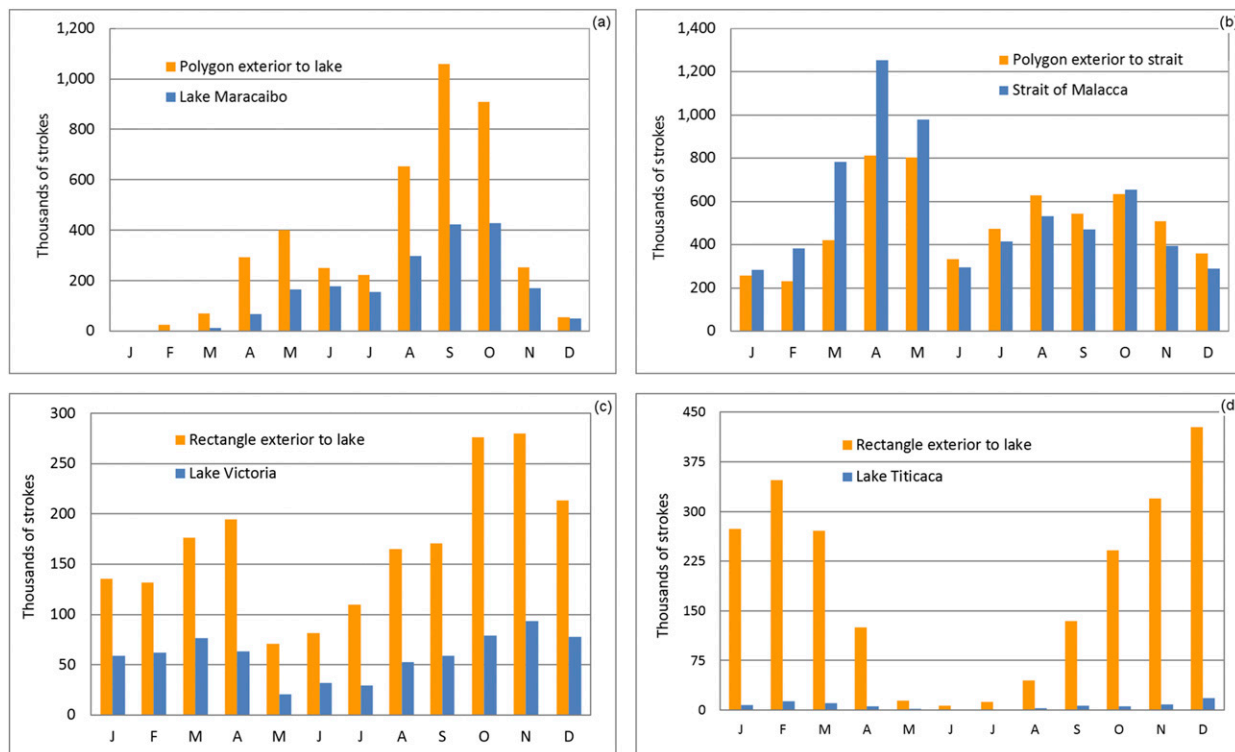


FIG. 3. Number of strokes by month over (a) Lake Maracaibo and polygon exterior to lake, (b) Strait of Malacca and polygon exterior to strait, (c) Lake Victoria and rectangle exterior to lake, and (d) Lake Titicaca and rectangle exterior to lake as indicated in Fig. 1.

the high terrain, resulting in relatively wet periods when the high is farther south and easterly flow is enhanced (Garreaud 1999).

6. Diurnal variations

The diurnal cycle of lightning over the four regions is shown from four different perspectives, as follows:

- Figure 4 shows the hourly percent contributions to the diurnal totals occurring within the day in all four regions with Fig. 4a showing the land areas surrounding the water bodies and Fig. 4b showing the overwater areas.
- Figure 5 shows stroke density maps for each region starting at midafternoon, midnight, and sunrise.
- Figure 6 shows the time of day with the maximum lightning frequency.
- Figure 7 indicates the diurnal cycle with Hovmöller cross sections over swaths through the center of the water bodies from southwest to northeast as shown in Fig. 1.

a. Combined diurnal time series

A combined analysis of lightning occurrence over and surrounding the four bodies of water is shown in Fig. 4. Both panels are expressed in percent of all lightning occurring within the day for each water body.

The lightning maxima over the landmasses (Fig. 4a) are nearly in phase between 1500 and 1700 LST. The land surrounding Lake Maracaibo actually exhibits the superposition of two peaks: one near 1600 LST that occurs outside of the low-level, swampy Catatumbo River valley; and a second peak associated with evening convection over the river valley itself. All other land areas have small amounts of lightning between 2000 and 1100 LST.

By contrast, the maxima in lightning frequency over water (Fig. 4b) are out of phase in the different locations. The nocturnal maxima over both Lake Maracaibo and the Strait of Malacca occur after midnight. Lake Victoria exhibits an increase of lightning frequency during the night, but the actual peak is delayed until after sunrise. By contrast, Lake Titicaca has its peak during the hours immediately after sunset.

b. Lake Maracaibo

Maps of the diurnal cycle (Fig. 5) in three selected time intervals (1500–1800, 0000–0300, and 0600–0900 LST) indicate how the daytime lightning maxima on the mountain slopes switch to a nighttime maximum over the water. During the first time period from 1500 to 1800 LST, stroke densities are large over the slopes of the high terrain as well as over the elevated plateau to the

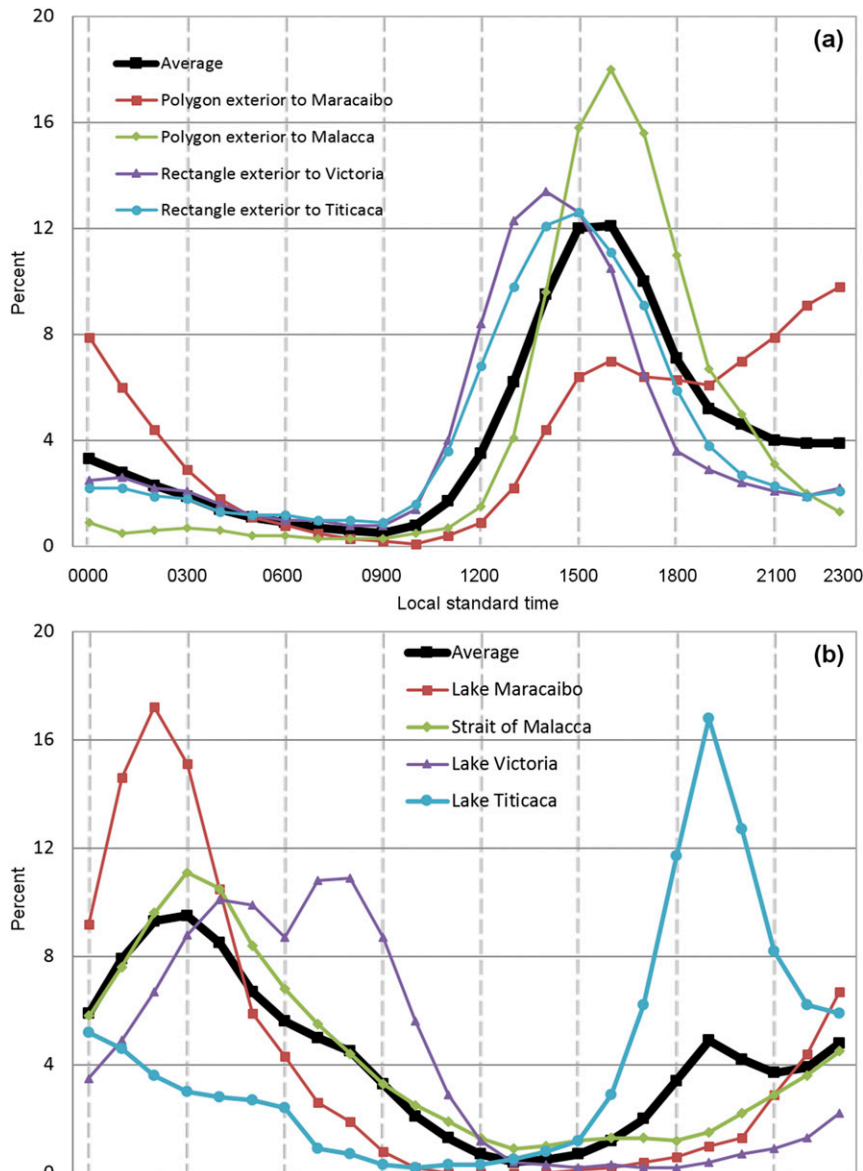


FIG. 4. Percent of lightning occurring within the day over (a) the surrounding four land areas and (b) over each lake and Strait of Malacca by hour of day in local solar time (LST).

northeast, while there is a distinct minimum over the water. Nine hours later from 0000 to 0300 LST, Lake Maracaibo has an enormous maximum. Lightning also persists into the early morning as well (0600–0900 LST).

Maximum stroke occurrence peaks near midnight over the southwest portion of the lake (Fig. 6a), then it is later at night to after sunrise over the northeast portion. Over most land areas, the most frequent time for a lightning maximum is from afternoon to early evening (1500–1900 LST). The afternoon lightning maxima along the flanks of the Sierra de Perijá and Eastern Cordillera ranges gradually migrate into the lower

altitudes of the Catatumbo River valley between 1900 and 2300 LST. This lightning maximum then either merges with or initiates the lightning maximum over the lake by 0200–0300 LST.

The Hovmöller cross section (Fig. 7a) indicates a lightning density maximum that peaks around 0200 LST. The combination of Figs. 6a and 7a suggests, however, that the space–time evolution may be dominated by the development of thunderstorms over the Catatumbo River valley to the west–southwest of the lake from about 1600 LST onward, leading into the nocturnal maximum over the lake itself. Muñoz et al. (2016) have described

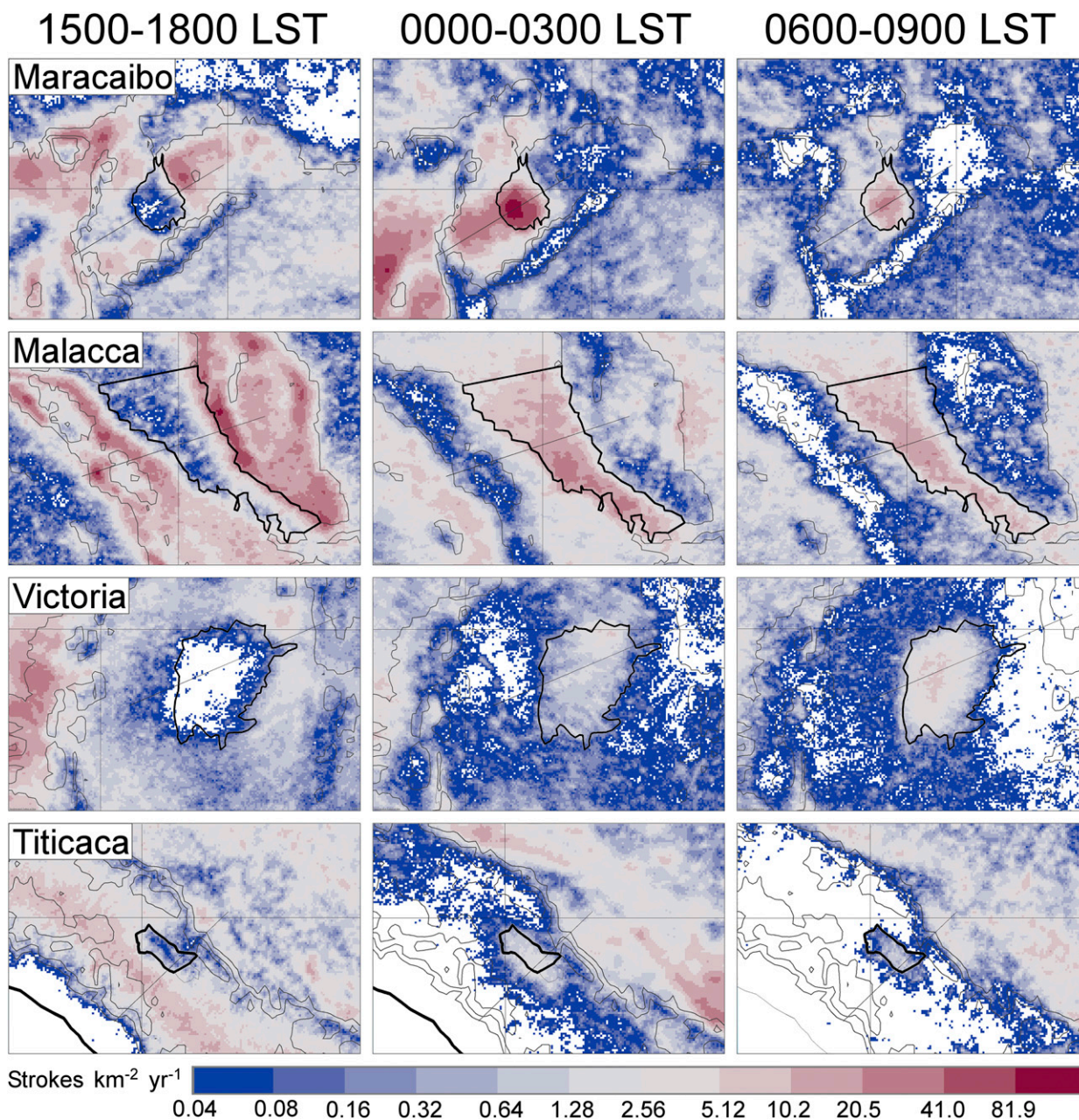


FIG. 5. (left to right) The 3-hourly maps of lightning over and in vicinity of (top to bottom) four water bodies at indicated LSTs. Terrain contours and water body outlines as in Fig. 2. Black southwest–northeast lines indicate locations of the cross sections in Fig. 7.

4- and 30-km Weather Research and Forecasting (WRF) Model simulations of the processes involved. A strong southwesterly directed low-level jet operates during the late afternoon and evening through meridional wind anomalies and establishes convergence along the terrain to the southwest of the lake. Cool outflows from the resulting convection apparently shift the convergence zone and convection maximum toward the Catatumbo River valley during the evening and eventually turn the

low-level wind to approximately alongshore (Albrecht et al. 2016), which may or may not assist in pushing the area of convergence to the lake during the middle of the night. In addition, it also appears as though the convection over the northeast shore of the lake in the late afternoon is loosely connected to the nocturnal maximum, perhaps via its own cool outflows, which would serve to reinforce the convergence zone established to the southwest of the lake during the evening.

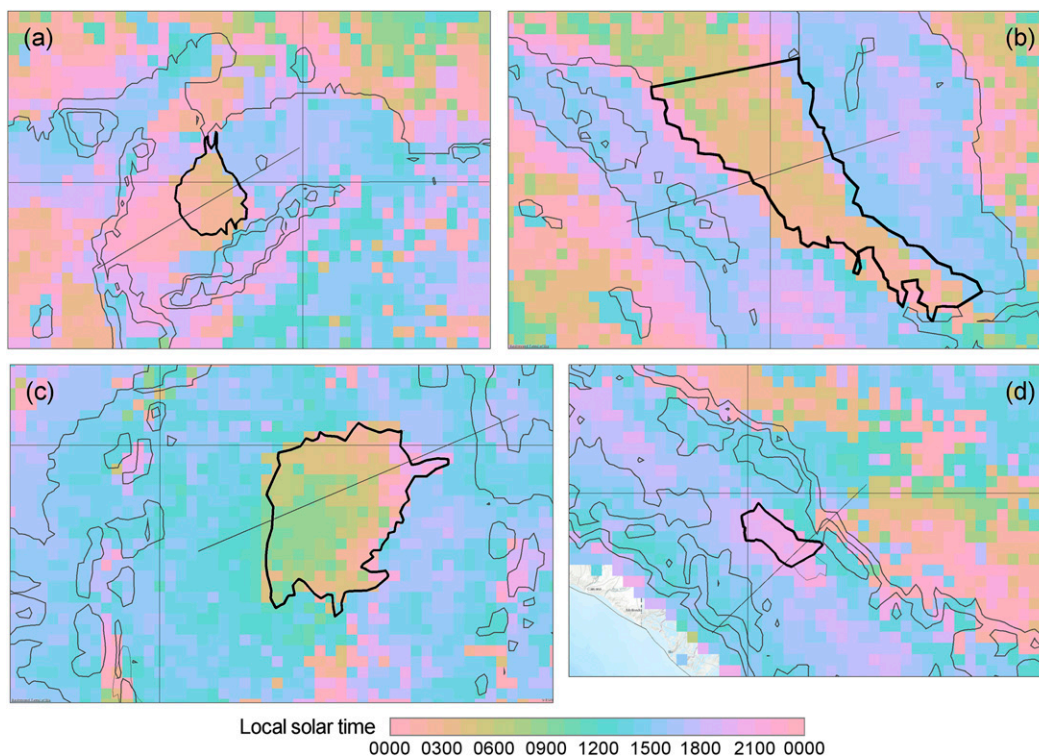


FIG. 6. Hour of day in LST with maximum lightning frequency in a $20 \text{ km} \times 20 \text{ km}$ grid for (a) Lake Maracaibo, (b) Strait of Malacca, (c) Lake Victoria, and (d) Lake Titicaca. Time is indicated by color bar. Terrain contours and water body outlines are as in Fig. 2. Black southwest–northeast lines indicate locations of the cross sections in Fig. 7.

c. Strait of Malacca

A maximum in stroke density over land surrounding the strait is apparent in the midafternoon in Fig. 5, while a strong maximum occurs over the strait during the night. The peak lightning occurrence is closer to midnight over the southeast portion of the strait (Fig. 6b), then it is later at night to after sunrise over the northwest portion. The cross section in Fig. 7b shows minimal lightning over water during the afternoon, then an overwater maximum after midnight into the early morning. There is some indication in Fig. 7b that the decaying maximum over the strait actually pushes onshore at about 1200 LST, perhaps reinforcing the sea-breeze circulations on both shores, or even launching them. The land surfaces between the mountains and coastlines on both sides clearly dominate lightning occurrence between 1500 and 1800 LST, as evident in the 3-hourly maps of Fig. 5. Between about 1900 and 2200 LST, the maximum on the Malaysian side then appears to blend into the eventual nocturnal maximum over water.

d. Lake Victoria

Maximum lightning frequency from 0000 to 0300 LST is over the northeastern corner of the lake

(Fig. 5), and then the lightning maximum progresses across the lake through the night into morning. Maxima after midnight are also very apparent over the larger Rift Valley lakes to the northwest and west (Fig. 6c). Nearly all of the surrounding areas have an afternoon maximum from 1400 to 1800 LST (Fig. 4a), while about half of the grid squares over the lake itself have no lightning at all from 1500 to 1800 LST (Fig. 5). The cross section (Fig. 7c) shows that the overwater maximum begins after midnight and then persist for many hours until nearly noon. There is evidence of propagation, on average, from northeast to southwest, although on any particular day, there may actually be a distinct break between afternoon convection over land and nocturnal convection over the lake. On average, Fig. 7c indicates that the afternoon maximum occurs between the Kenyan highlands and the northeast shore of the lake and then extends into the nocturnal maximum over the lake, and ends with an early afternoon maximum to the southwest of the lake. Modeling studies by Anyah et al. (2006) show sensitivity of the diurnal cycle to the setup of the lake-breeze front to the northeast of the lake in the afternoon, as well as high sensitivity of the overall seasonal cycle of precipitation in the region to moisture arriving from the

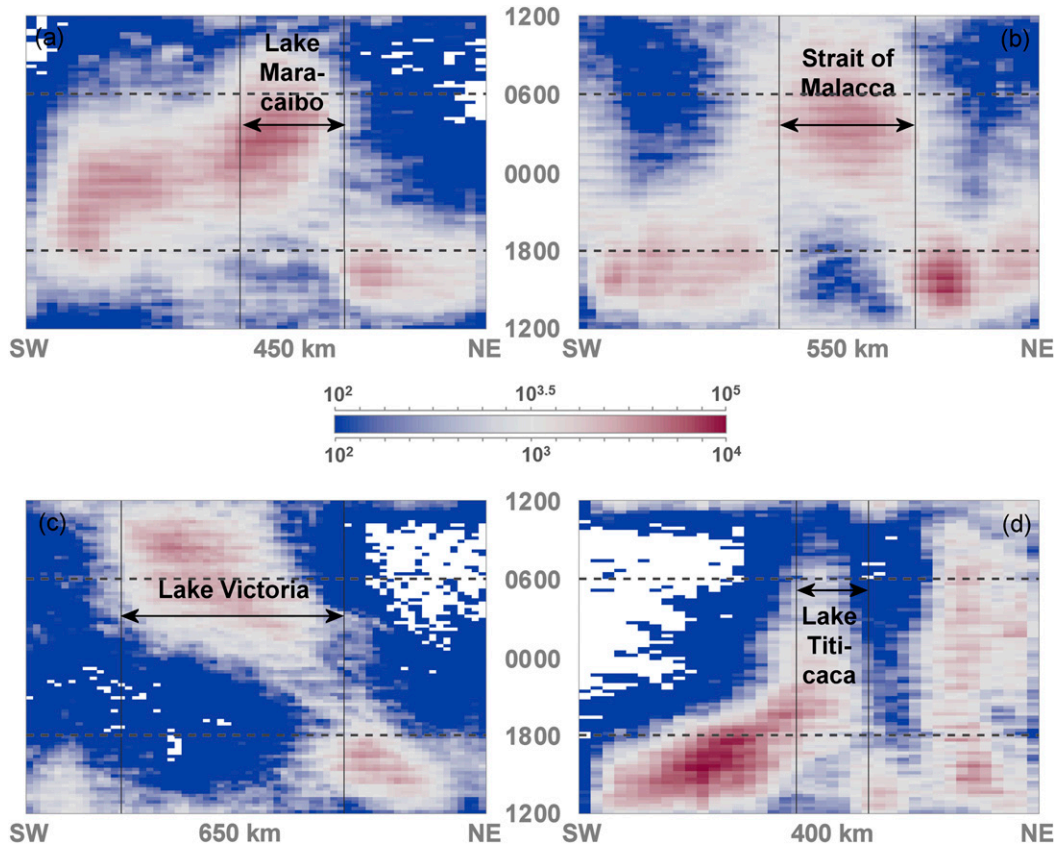


FIG. 7. Hovmöller diagrams along cross sections from southwest to northeast across the four water bodies as indicated by dashed lines in Figs. 1, 2, 5, and 6. Time of day (LST) is indicated by the vertical scale in the center; dashed black lines are sunrise and sunset. Color shading shows the number of strokes (on logarithmic scale), with a range of 10^2 – 10^5 on the top for Lake Maracaibo and the Strait of Malacca, and a range of 10^2 – 10^4 on the bottom for Lakes Victoria and Titicaca. All diagrams use bins of 10 km in the distance dimension by 15 min in the time-of-day dimension. The total lengths of cross sections are between 450 and 650 km (indicated at the bottom of each panel), and water body cross sections are 100–200 km wide (indicated by the vertical black lines).

western Indian Ocean. The Kenyan highlands evidently partially impede easterly flow from the Indian Ocean, and heating of this mountain range also draws the lake-breeze front deeper into Kenya, setting up the convergence zone that creates the local maximum in thunderstorm activity along the eastern shore of the lake between 1500 and 1800 LST. We suspect that the collapse of that convection then leads to a cool easterly outflow that penetrates deep into the west side of the lake where the water temperature is warmer (Song et al. 2004; Anyah 2005). This leads to an absolute maximum in lightning density that is displaced to the west and occurs after 0600 LST, consistent with Fig. 5 and with the diurnal cycle of cold cloud tops shown by Chamberlain et al. (2014). Curiously, Bürgesser et al. (2013) found maximum lightning density over the northern and central parts of the lake, with a two-peaked time distribution, which is inconsistent with

the satellite and precipitation studies of the area and with the present results.

e. Lake Titicaca

Maximum lightning begins in the evening and extends after midnight over the center of the lake (Fig. 6d). Maxima after midnight are also apparent over lower elevations to the east. Nearly all other land areas have peak lightning occurrence between noon and sunset. There is a progression from a near-noon maximum over high terrain along the southwest and northeast flanks of the lake toward a later afternoon peak along a northwest–southeast axis through the lake itself (Fig. 6d).

As noted above, the nighttime maximum is earlier than over the three lower-altitude water bodies in this study, specifically between 1900 and 2300 LST. The cross section in Fig. 7d shows that convection over the

surrounding high terrain both to the southwest and northeast ramps up strongly and suddenly near 1200 LST. The maximum to the southwest (left) of the lake drifts slowly toward the northeast as the afternoon progresses, consistent with the 3-hourly densities shown in Fig. 5. As the land-side thunderstorms decay after 1800 LST, the nearshore and overlake maximum reaches its peak shortly after sunset. Although the peak lightning density over the lake occurs prior to midnight, Fig. 7d shows that a weak overwater maximum persists after midnight until shortly after sunrise, with a tendency to be displaced toward the southwest shore where the water depth is less than 200 m and average temperatures are closer to 15°C. The persistence of the maximum all night is consistent with the findings of Giovannetone and Barros (2009), who looked at TRMM precipitation features having reflectivity of at least 20 dBZ and 85-GHz polarization-corrected temperature of 250 K or less. They noted a distinct local maximum in such features, representative of convective clouds containing ice, over Lake Titicaca during the 0000–0600 LST time period, as well as a distinct minimum in these features directly over the lake between 1200 and 1800 LST. They attributed the nocturnal maximum to downslope flow from the surrounding terrain, but not explicitly to cool outflow from the preceding afternoon convection over the terrain. However, it is important to note that they did not consider the 1800–0000 UTC time period, when the absolute maximum in lightning density occurs over the lake.

7. Discussion and conclusions

The foregoing perspectives on the diurnal cycle highlight the three common features of these four water bodies noted in section 1: 1) prominent nocturnal maxima in lightning density over water that are sustained all night and into the following morning, 2) delayed maturation of the nocturnal maxima at all sites but Lake Titicaca, and 3) significant differences in the local time of the four nocturnal maxima although the lightning maxima on the surrounding land areas all occur between 1500 and 1700 LST. As noted in the literature review, we suspect that the primary emphasis on lake–sea and land breezes in the prior literature obscures and fails to bring attention to some other critical factors.

The sustainment of lightning all night, even at the relatively cold, high-altitude site of Lake Titicaca, suggests that input of sensible and latent heat from the water, which is warmer at night than surrounding land, is potentially the most obvious factor aside from low-level circulation. However, the broad Magdalena Valley of northern Colombia, located a short distance to the

southwest of Lake Maracaibo, also has a prominent nocturnal maximum in precipitation (Mapes et al. 2003b) as well as a nocturnal maximum in lightning (Albrecht et al. 2016), but no body of water. Similarly, other parts of the Amazon and Congo basins also have significant nocturnal lightning activity. Thus, the water body itself is not a necessary ingredient in the generation of a nocturnal maximum in convective activity. Therefore, it may be the case that a low-level circulation, in either the form of outflow from afternoon land-based convection or downslope breezes or a combination of both, initiates the overwater convection at night, then evolves into a self-sustaining meso- α -scale circulation during the remainder of the night. That is, subsidence outside the thunderstorms over water reinforces the downslope breezes, which in turn then reinforces the nocturnal convection until after sunrise, when the upslope breeze develops over the mountain slopes. This notion is similar in some respects to the conceptual summary of another region, the south slopes of the Himalayas, which has a nocturnal maximum in precipitation (Barros et al. 2004). They proposed a sequence of stationary nocturnal vertical circulations, abetted by cool outflow early, and subsequently sustained during the night by the interaction of midlevel winds and orographic gravity waves with specific ridges and valleys.

The degree to which downslope breezes, as opposed to cool outflow from afternoon land-based thunderstorms, instigate nocturnal thunderstorms over water may be testable by examining how often there are nights with thunderstorms over water without land-based thunderstorms the preceding afternoon. We defer that analysis to future work. However, there is evidence in the literature that the low-altitude circulation may be dominated by the convergence of cool outflow from convection on land during the afternoon. At the Strait of Malacca, shipborne measurements by Fujita et al. (2010) showed cool offshore flow from both sides of the strait, with temperature differentials of 4°–5°C. According to a “dry” simulation performed by Fujita et al. (2010), katabatic winds alone would not have such a large temperature differential, consistent with Mapes et al. (2003a) and indicating the likely dominance of convective outflow. Additional sensitivity studies of the type conducted by Fujita et al. (2010) and Anyah et al. (2006) may reveal whether subtle differences in the timing of the lake–land temperature contrast and overwater convergence are attributable to downslope breezes versus outflow from afternoon thunderstorms over land, but these are outside the scope of the present paper.

If pure low-level circulation from land to water were the dominant factor in the nocturnal convection over

water, then we might anticipate that, on average, the maximum lightning frequency at all sites might occur shortly after sunset, when the atmosphere remains warm and unstable and offshore-directed circulations are first established. Instead, we observe significant delays in the time of the lightning maxima at the three lower-altitude sites in this study. In addition, as noted above with respect to Lake Maracaibo, the surface wind climatology presented by [Albrecht et al. \(2016\)](#) shows an alongshore component at night, making it unclear whether or not low-level convergence is dominant. Such observations suggest that destabilization of the midtroposphere may also have an important role. This destabilization could have a number of sources. [Mapes et al. \(2003a\)](#) identified a gravity wave that acted to cool the area around the 800-mb level over northwestern South America, but it should be noted that they also showed, but did not specifically identify, a second area of nocturnal cooling at around the 600-mb level. Lake Titicaca is a unique case: being at roughly 650 mb, it can serve as its own source of midtropospheric destabilization by direct injection of sensible and latent heat at that altitude. In this context, it is also important to note that Lake Titicaca is essentially cut off from all low-level moisture sources but is able to yield an all-night lightning maximum. Those unique features may explain why its lightning maximum occurs shortly after sunset in contrast with the other sites.

Although the overall patterns of behavior may be broadly consistent with the coastal regime of convective diurnal cycles identified by [Kikuchi and Wang \(2008\)](#), we hypothesize that the phase differences of the nocturnal maxima between the four sites probably result from site-specific combinations of the aforementioned factors. For instance, Lake Victoria is warmest near its west-southwest shore, but given the northeast–southwest propagation of thunderstorms from the Kenyan highlands in the afternoon across the lake at night, the thunderstorms do not reach the southwest side until morning, perhaps explaining why the peak lightning density at Lake Victoria occurs in the early morning. By contrast, the lightning maximum over Lake Maracaibo is slightly earlier on the southwest side than to the northeast, and we note an evening maximum along the river valley to the southwest of the lake that either instigates or blends into the nighttime maximum over the lake.

While nocturnal lightning density maxima are found over certain land areas, note that the converse also exists: Lake Okeechobee, a significant water body at 26°N in the United States, experiences no nocturnal lightning density maximum. Instead, there is a minimum in lightning occurrence over the lake compared with large

densities over surrounding heated land ([Holle 2014](#)). There is warm water in summer (30°C), and the lake is essentially at sea level, similar to Lake Maracaibo and the Strait of Malacca, but there is no elevated topography surrounding the lake. Thus, an additional low- to midaltitude factor must be a significant terrain gradient, perhaps assisting the convergence either via convective outflow from the afternoon storms on land and/or a downslope breeze circulation. Lake Okeechobee is also much smaller and at a higher latitude than the other water bodies in this study, and located on a peninsula where sea breezes are very strong in summer.

It is important to note that the diurnal cycle is just one component, albeit an important one, of the overall climatology of thunderstorms in the areas of these four water bodies, as well as the tropics in general. For instance, [Laing et al. \(2011\)](#) have shown that convection over all of equatorial Africa, including the Lake Victoria region, is modulated on weekly time scales by equatorial Kelvin waves, as well as on longer time scales by the Madden–Julian oscillation (MJO). The MJO also has an important role in regulating thunderstorm activity over the entire Maritime Continent, not only the Strait of Malacca ([Virts et al. 2013b](#)).

This study raises a wide variety of unresolved issues. Future studies of these four water bodies and their surroundings might seek to investigate how the nondiurnal cycles affect or modulate the occurrence of lightning over the water versus over the surrounding terrain, and whether or not these cycles alter the general patterns presented in this study. Since these are four different locations with differing regimes of large-scale and local flow patterns, it will be necessary to conduct studies of each lake or strait separately, despite the fact that all four water bodies have nighttime maxima in lightning following afternoon maxima over surrounding elevated terrain.

In conclusion, the diurnal cycles of lightning activity were examined over and around four large tropical water bodies that are surrounded by significant terrain gradients of various configurations. It was found that all four water bodies have nocturnal maxima in lightning density that follow large afternoon lightning densities over the surrounding terrain. The key observations, in our view, are that 1) lightning activity is sustained all night at all four sites, 2) there is a substantial delay between the afternoon peak in lightning activity over the surrounding land areas and the nocturnal maxima over water at all sites except Lake Titicaca, and 3) there is significant phase variation in the nocturnal maxima over water, even though the afternoon maxima over land at all four locations are very well phase-matched and occur between 1500 and 1700 LST.

The low-level circulation may initiate nighttime overwater convection, due to outflows from afternoon land-based convection and/or from downslope breezes, and evolve into a self-sustaining meso- α -scale circulation. There are significant time delays of the lightning maxima at the three lower-altitude sites, suggesting that destabilization of the midtroposphere may be important. Phase differences of the nocturnal maxima among the four sites probably result from site-specific combinations of these factors.

Acknowledgments. The authors greatly appreciate the careful, extensive preparation of the lightning data and mapping of strokes by Mr. William Brooks of Vaisala in Tucson, Arizona. The comprehensive and constructive comments of three reviewers greatly assisted in organizing and clarifying the results of the study.

REFERENCES

- Abarca, S. F., K. L. Corbosiero, and T. J. Galarneau Jr., 2010: An evaluation of the Worldwide Lightning Location Network (WLLN) using the National Lightning Detection Network (NLDN) as ground truth. *J. Geophys. Res.*, **115**, D18206, doi:10.1029/2009JD013411.
- Albrecht, R. I., S. J. Goodman, D. E. Buechler, R. J. Blakeslee, and H. J. Christian, 2016: Where are the lightning hotspots on Earth? *Bull. Amer. Meteor. Soc.*, **97**, 2051–2068, doi:10.1175/BAMS-D-14-00193.1.
- Anyah, R. O., 2005: Modeling the variability of the climate system over Lake Victoria basin. Ph.D. thesis, Dept. of Marine, Earth and Atmospheric Sciences, North Carolina State University, 307 pp., <https://repository.lib.ncsu.edu/handle/1840.16/3820>.
- , F. H. M. Semazzi, and L. Xie, 2006: Simulated physical mechanisms associated with climate variability over Lake Victoria basin in East Africa. *Mon. Wea. Rev.*, **134**, 3588–3609, doi:10.1175/MWR3266.1.
- Barros, A. P., G. Kim, E. Williams, and S. W. Nesbitt, 2004: Probing orographic controls in the Himalayas during the monsoon using satellite imagery. *Nat. Hazards Earth Syst. Sci.*, **4**, 29–51, doi:10.5194/nhess-4-29-2004.
- Berghuis, E. P. D., 1995: Salinity in Lake Maracaibo. M.S. thesis, Faculty of Civil Engineering Hydraulic and Geotechnical Engineering Division, and Delft Hydraulics Estuaries and Seas Division, Delft University of Technology, Delft, Netherlands, 74 pp., <https://repository.tudelft.nl/islandora/object/uuid:69df939d-2d36-494b-90b9-e51a1f0bee1c>.
- Boccippio, D. J., W. J. Koshak, and R. J. Blakeslee, 2002: Performance assessment of the optical transient detector and lightning imaging sensor. Part I: Predicted diurnal variability. *J. Atmos. Oceanic Technol.*, **19**, 1318–1332, doi:10.1175/1520-0426(2002)019<1318:PAOTOT>2.0.CO;2.
- Bürgesser, R. E., M. G. Nicora, and E. E. Avila, 2012: Characterization of the lightning activity of “Relampago del Cata-tumbo.” *J. Atmos. Sol.-Terr. Phys.*, **77**, 241–247, doi:10.1016/j.jastp.2012.01.013.
- , —, and —, 2013: Spatial and time distribution of the flash rate over tropical Africa. *J. Atmos. Sol.-Terr. Phys.*, **94**, 41–48, doi:10.1016/j.jastp.2012.12.025.
- Chamberlain, J. M., C. L. Bain, D. F. A. Boyd, K. McCourt, T. Butcher, and S. Palmer, 2014: Forecasting storms over Lake Victoria using a high resolution model. *Meteor. Appl.*, **21**, 419–430, doi:10.1002/met.1403.
- Delclaux, F., A. Coudrain, and T. Condom, 2007: Evaporation estimation of Lake Titicaca: A synthesis review and modeling. *Hydrol. Processes*, **21**, 1664–1677, doi:10.1002/hyp.6360.
- Frei, C., and C. Schär, 1998: A precipitation climatology of the Alps from high-resolution rain-gauge observations. *Int. J. Climatol.*, **18**, 873–900, doi:10.1002/(SICI)1097-0088(19980630)18:8<873::AID-JOC255>3.0.CO;2-9.
- Fujita, M., F. Kimura, and M. Yoshizaki, 2010: Morning precipitation peak over the Strait of Malacca under a calm condition. *Mon. Wea. Rev.*, **138**, 1474–1486, doi:10.1175/2009MWR3068.1.
- Garreaud, R. D., 1999: Multiscale analysis of the summertime precipitation over the central Andes. *Mon. Wea. Rev.*, **127**, 901–921, doi:10.1175/1520-0493(1999)127<0901:MAOTSP>2.0.CO;2.
- Giovannetone, J. P., and A. P. Barros, 2009: Probing regional orographic controls of precipitation and cloudiness in the central Andes using satellite data. *J. Hydrometeorol.*, **10**, 167–182, doi:10.1175/2008JHM973.1.
- Holle, R. L., 2014: Diurnal variations of NLDN-reported cloud-to-ground lightning in the United States. *Mon. Wea. Rev.*, **142**, 1037–1052, doi:10.1175/MWR-D-13-00121.1.
- Houze, R. A., Jr., 2012: Orographic effects on precipitating clouds. *Rev. Geophys.*, **50**, RG1001, doi:10.1029/2011RG000365.
- Jones, C., and L. M. V. Carvalho, 2002: Active and break phases in the South American monsoon system. *J. Climate*, **15**, 905–914, doi:10.1175/1520-0442(2002)015<0905:AABPIT>2.0.CO;2.
- Kikuchi, K., and B. Wang, 2008: Diurnal precipitation regimes in the global tropics. *J. Climate*, **21**, 2680–2696, doi:10.1175/2007JCL2051.1.
- Laing, A. G., R. E. Carbone, and V. Levizzani, 2011: Cycles and propagation of deep convection over equatorial Africa. *Mon. Wea. Rev.*, **139**, 2832–2853, doi:10.1175/2011MWR3500.1.
- López, R. E., and R. L. Holle, 1986: Diurnal and spatial variability of lightning activity in northeastern Colorado and central Florida during the summer. *Mon. Wea. Rev.*, **114**, 1288–1312, doi:10.1175/1520-0493(1986)114<1288:DASVOL>2.0.CO;2.
- MacGorman, D. R., T. Filiaggi, R. L. Holle, and R. A. Brown, 2007: Cloud-to-ground lightning flash rates relative to VIL, maximum reflectivity, cell height, and cell isolation. *J. Lightning Res.*, **1**, 132–147.
- Mach, D. M., H. J. Christian, R. J. Blakeslee, D. J. Boccippio, S. J. Goodman, and W. L. Boeck, 2007: Performance assessment of the Optical Transient Detector and Lightning Imaging Sensor. *J. Geophys. Res.*, **112**, D09210, doi:10.1029/2006JD007787.
- Mallick, S., and Coauthors, 2014a: Evaluation of the GLD360 performance characteristics using rocket-and-wire triggered lightning data. *Geophys. Res. Lett.*, **41**, 3636–3642, doi:10.1002/2014GL059920.
- , and Coauthors, 2014b: Performance characteristics of the NLDN for return strokes and pulses superimposed on steady currents, based on rocket-triggered lightning data acquired in Florida in 2004–2012. *J. Geophys. Res. Atmos.*, **119**, 3825–3856, doi:10.1002/2013JD021401.
- Mapes, B. E., T. T. Warner, and M. Xu, 2003a: Diurnal patterns of rainfall in northwestern South America. Part III: Diurnal gravity waves and nocturnal convection offshore. *Mon. Wea. Rev.*, **131**, 830–844, doi:10.1175/1520-0493(2003)131<0830:DPORIN>2.0.CO;2.
- , —, —, and A. J. Negri, 2003b: Diurnal patterns of rainfall in northwestern South America. Part I: Observations

- and context. *Mon. Wea. Rev.*, **131**, 799–812, doi:[10.1175/1520-0493\(2003\)131<0799:DPORIN>2.0.CO;2](https://doi.org/10.1175/1520-0493(2003)131<0799:DPORIN>2.0.CO;2).
- Muñoz, A. G., J. Díaz Lobatón, X. Chourio, and M. J. Stock, 2016: Seasonal prediction of lightning activity in north-western Venezuela: Large-scale versus local drivers. *Atmos. Res.*, **172–173**, 147–162, doi:[10.1016/j.atmosres.2015.12.018](https://doi.org/10.1016/j.atmosres.2015.12.018).
- National Geospatial-Intelligence Agency, 1988: Lago de Maracaibo. Chart 24481, Defense Mapping Agency, <http://www.costadevenezuela.org/cartas/lagomg.pdf>.
- NOAA/OAR/ESRL PSD, 2017: Weekly SST totals for the past 52 weeks. NOAA/OAR/ESRL Physical Sciences Division, Boulder, CO, accessed 8 April 2017, <https://www.esrl.noaa.gov/psd/map/clim/sst.anim.year.html>.
- Poelman, D. R., W. Schulz, and C. Vergeiner, 2013: Performance characteristics of distinct lightning detection networks covering Belgium. *J. Atmos. Oceanic Technol.*, **30**, 942–951, doi:[10.1175/JTECH-D-12-00162.1](https://doi.org/10.1175/JTECH-D-12-00162.1).
- Pohjola, H., and A. Mäkelä, 2013: The comparison of GLD360 and EUCLID lightning location systems in Europe. *Atmos. Res.*, **123**, 117–128, doi:[10.1016/j.atmosres.2012.10.019](https://doi.org/10.1016/j.atmosres.2012.10.019).
- Rudlosky, S. D., and D. T. Shea, 2013: Evaluating WWLLN performance relative to TRMM/LIS. *Geophys. Res. Lett.*, **40**, 2344–2348, doi:[10.1002/grl.50428](https://doi.org/10.1002/grl.50428).
- Said, R., and M. J. Murphy, 2016: GLD360 upgrade: Performance analysis and applications. *24th Int. Lightning Detection Conf. & Sixth Int. Lightning Meteorology Conf.*, San Diego, CA, Vaisala, 8 pp., <https://my.vaisala.net/en/events/ildcilmc/archive/Pages/ILDCILMC-2016-Archive.aspx>.
- , M. B. Cohen, and U. S. Inan, 2013: Highly intense lightning over the oceans: Estimated peak currents from global GLD360 observations. *J. Geophys. Res. Atmos.*, **118**, 6905–6915, doi:[10.1002/jgrd.50508](https://doi.org/10.1002/jgrd.50508).
- Song, Y., F. H. M. Semazzi, L. Xie, and L. J. Ogallo, 2004: A coupled regional climate model for the Lake Victoria basin of East Africa. *Int. J. Climatol.*, **24**, 57–75, doi:[10.1002/joc.983](https://doi.org/10.1002/joc.983).
- Stolz, D. C., S. A. Rutledge, and J. R. Pierce, 2015: Simultaneous influences of thermodynamics and aerosols on deep convection and lightning in the tropics. *J. Geophys. Res. Atmos.*, **120**, 6207–6231, doi:[10.1002/2014JD023033](https://doi.org/10.1002/2014JD023033).
- Sun, X., L. Xie, F. Semazzi, and B. Liu, 2015: Effect of lake surface temperature on the spatial distribution and intensity of the precipitation over the Lake Victoria Basin. *Mon. Wea. Rev.*, **143**, 1179–1192, doi:[10.1175/MWR-D-14-00049.1](https://doi.org/10.1175/MWR-D-14-00049.1).
- Venugopal, V., K. Virts, J. Sukhatme, J. M. Wallace, and B. Chattopadhyay, 2016: A comparison of the fine-scale structure of the diurnal cycle of tropical rain and lightning. *Atmos. Res.*, **169**, 515–522, doi:[10.1016/j.atmosres.2015.09.004](https://doi.org/10.1016/j.atmosres.2015.09.004).
- Virts, K. S., J. M. Wallace, M. L. Hutchins, and R. H. Holzworth, 2013a: Highlights of a new ground-based, hourly global lightning climatology. *Bull. Amer. Meteor. Soc.*, **94**, 1381–1391, doi:[10.1175/BAMS-D-12-00082.1](https://doi.org/10.1175/BAMS-D-12-00082.1).
- , —, —, and —, 2013b: Diurnal lightning variability over the Maritime Continent: Impact of low-level winds, cloudiness, and the MJO. *J. Atmos. Sci.*, **70**, 3128–3146, doi:[10.1175/JAS-D-13-021.1](https://doi.org/10.1175/JAS-D-13-021.1).